Helical Packing

DOI: 10.1002/anie.201403565

Helical Packing of Nanoparticles Confined in Cylindrical Domains of a Self-Assembled Block Copolymer Structure**

Sunita Sanwaria, Andriy Horechyy, Daniel Wolf, Che-Yi Chu, Hsin-Lung Chen, Petr Formanek, Manfred Stamm, Rajiv Srivastava, and Bhanu Nandan**

Abstract: *Theoretical models predict that a variety of self-assembled structures of closely packed spherical particles may result when they are confined in a cylindrical domain. In the present work we demonstrate for the first time that the polymer-coated nanoparticles confined in the self-assembled cylindrical domains of a block copolymer pack in helical morphology, where we can isolate individual fibers filled with helically arranged nanoparticles. This finding provides unique possibilities for fundamental as well as application-oriented research in similar directions.*

The self-assembly of block copolymers (BCP) has been an area of intense investigation for more than two decades now. The interest in these polymers is based primarily on their ability to self-assemble into various periodic nanostructures depending on the BCP composition and block ratios.[1] Owing to the ordered nanoscale morphologies formed by the block copolymers and the chemically distinct nature of the blocks constituting the copolymer, they can be used as templates to host and direct the assembly of externally added additives such as inorganic nanoparticles (NPs). A number of studies, both theoretical and experimental, have been conducted in this direction, with a focus on the controlled localization of nanoparticles in the microphase-separated structure of block copolymers.[2] Although diverse methods to fabricate NP/BCP mixtures and control the nanoparticle location within the BCP matrix are well established and widely described, most of the literature reports do not describe the structures formed by the nanoparticles themselves, revealing in most cases random particle arrangements within host domain of self-assembled BCP matrix. However, theoretical work on NP/BCP systems have predicted that the spherical nanoparticles with preferential attraction to the minority block of the BCP can indeed self-assemble within the host domain and generate a variety of one-, two-, or three- dimensional ordered morphologies.[3] One of the interesting morphologies predicted is the helical packing of nanoparticles in cylindrical domains of block copolymers which, however, has never been observed experimentally. The helical assemblies of nanoparticles are of interest since in such materials the nanoparticle properties are superimposed with those originating from the helical symmetry of the structure. For instance, both experimental and theoretical studies provide clear evidence that helical structures of plasmonic nanoparticles display the optical circular dichroism (CD)[4] often observed for chiral molecules. In the present work, we report on the experimentally observed helical packing of silver nanoparticles (AgNPs) confined in the cylindrical domains of a polystyrene-*block*-poly(4-vinylpyridine) (PS-b-P4VP) diblock copolymer. To our knowledge, this is the first time that such helical superstructures of nanoparticles have been found in the self-assembled domains of block copolymers.

AgNPs stabilized with a polystyrene shell had a core diameter of about 6.9 nm as obtained by transmission electron microscopy (TEM). The PS-b-P4VP block copolymer used had a molecular weight of 59000 g mol^{-1}, where the volume fraction of PS block was roughly 0.3. The composition of the block copolymer corresponds to the cylindrical morphology in the block copolymer phase diagram with cylinders formed by the minority PS block embedded in P4VP matrix. The AgNP/PS-b-P4VP composites were prepared by mixing the two components in chloroform and subsequently the solvent was allowed to evaporate very slowly to produce the bulk sample.

Figure 1 shows the small-angle X-ray scattering (SAXS) results for the chloroform-cast neat PS-b-P4VP sample and a sample that was loaded with 10 wt % of AgNP. The SAXS intensity profile of the neat block copolymer shows a strong primary peak at $q \approx 0.13$ nm^{-1} and a higher order peak. The ratio of the two peak positions is $1:\sqrt{7}$, suggesting hexagonally packed cylindrical morphology with cylinders composed of the minority PS blocks. The SAXS intensity profile of the AgNP/PS-b-P4VP composite sample displays two weak peaks in the low-q region attributed to the cylindrical morphology of BCP, as we confirmed later using TEM. Due to the domain swelling after accommodation of nanoparticles, the expected and more intense primary scattering peak originating from

[*] S. Sanwaria, Prof. Dr. R. Srivastava, Prof. Dr. B. Nandan
Department of Textile Technology
Indian Institute of Technology Delhi
Hauz Khas, New Delhi 110016 (India)
E-mail: nandan@textile.iitd.ac.in
Dr. A. Horechyy, Dr. P. Formanek, Prof. Dr. M. Stamm
Leibniz Institut fur Polymerforschung Dresden e.V.
Hohe Strasse 6, 01069 Dresden (Germany)
E-mail: horechyy@ipfdd.de
Dr. D. Wolf
Institute of Structural Physics, Triebenberg Laboratory
Technische Universität Dresden
01062 Dresden (Germany)
Dr. C.-Y. Chu, Prof. Dr. H.-L. Chen
Department of Chemical Engineering
National Tsing-Hua University, Hsinchu 30013 (Taiwan)

[**] This research was supported by a grant from the Department of Science and Technology, India (RP02799) and by the DFG and BMBF.

Supporting information for this article is available on the WWW under http://dx.doi.org/10.1002/anie.201403565.

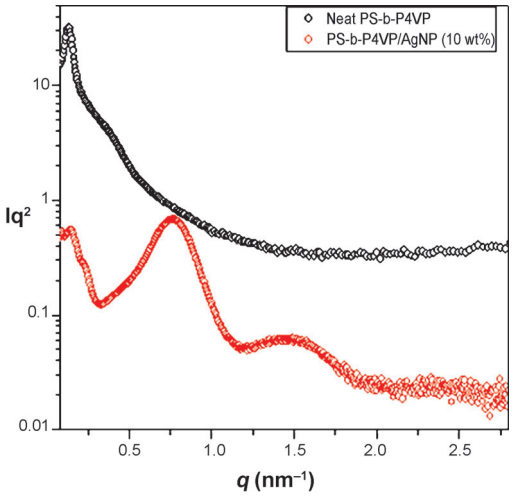

Figure 1. SAXS intensity profile of the neat block copolymer and its composite containing 10 wt% AgNPs.

BCP cylindrical morphology shifted to a lower q value with respect to that of neat BCP, which is beyond the limit of the instrument used. However, the ratio of the two peak positions observed in the SAXS profile can be scaled as $\sqrt{3}:\sqrt{7}$, indicating that the hexagonally packed cylindrical morphology of the BCP is retained, as revealed later by TEM. Next, an additional strong scattering peak at $q \approx 0.74\ \mathrm{nm}^{-1}$ appeared which plausibly originated from the close packing of nanoparticles inside the PS cylinders. Furthermore, the broad peaks in the high-q region resulted from the intraparticle scattering of individual nanoparticles.

Figure 2 shows the TEM images of the ultramicrotomed AgNP/PS-b-P4VP composite bulk sample recorded at the regions with parallel and perpendicular orientation to the cylindrical domain axis. Due to the presence of the PS shell, the nanoparticles were expected to be localized in the cylindrical domains of the BCP constituted of the minority PS block. Indeed, this is clearly evident in the TEM images where the AgNPs were almost exclusively present in the cylinder domains. But the most interesting observation was

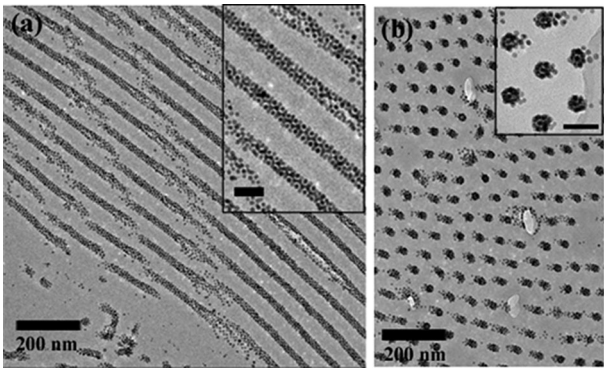

Figure 2. TEM images of self-assembled morphologies formed in an AgNP/PS-b-P4VP sample loaded with 10 wt% AgNPs: a) view along the plane of the PS cylinder axis, b) view normal to the plane of PS cylinder axis. Scale bars of the inset images correspond to 50 nm.

the closely packed structure of AgNPs within the cylinder where the NPs arrange in an ordered symmetry.

To better resolve the closely packed structure of the AgNPs, we isolated the PS cylindrical domains loaded with the AgNPs as individual nanofibers (NFs) by treating the bulk sample with a P4VP-selective solvent, that is, methanol. The details of the procedure have been reported in our previous work.[5] Figure 3 shows the TEM image of an isolated single NF with AgNPs incorporated within PS core and the shell composed of collapsed P4VP chains.

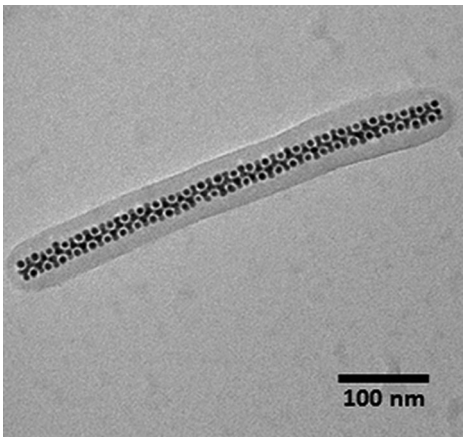

Figure 3. TEM image of a single NF isolated from the AgNP/PS-b-P4VP composite. The closely packed ordered structure of AgNPs is clearly evident from the TEM image.

The closely packed ordered structure of AgNPs in the isolated nanofibers is quite clear. The exact nature of the ordered three-dimensional (3D) structure was resolved using TEM imaging combined with an electron tomography technique[6] on an isolated NF loaded with AgNPs (Figure 4).

The 3D reconstruction of AgNP packing inside the nanofiber reveals a central chain of AgNPs along the long axis of the NF surrounded by a stack of rings of five nanoparticles, whereby adjacent rings are twisted 36° with respect to each other. This twist of adjacent particle layers gives rise to a spiral or helical NP arrangement, where the central nanoparticle chain is surrounded by five helical chains: One such chain is highlighted in red in Figure 4. The helical packing of nanoparticles was observed in a wide range of AgNP concentrations from 2 to 15 wt % with respect to the block copolymer.

It is well known that in NP/BCP composites, the distribution of NPs depends on a complex interplay between the enthalpic and entropic factors, which are associated with the polymer/NP interaction and with the chain deformation in order to accommodate the nanoparticles within a domain, respectively. The preferred interaction between the nanoparticles and particular block is the enthalpic driving force to localize them exclusively in one of the domains. The size of the nanoparticle as well as characteristics of the particle-stabilizing polymer shell (e.g. chemical properties, molecular weight, polymer grafting density, etc.) dictate whether the nanoparticles will be homogenously distributed throughout the host domain, localized at the domain interface, or forming

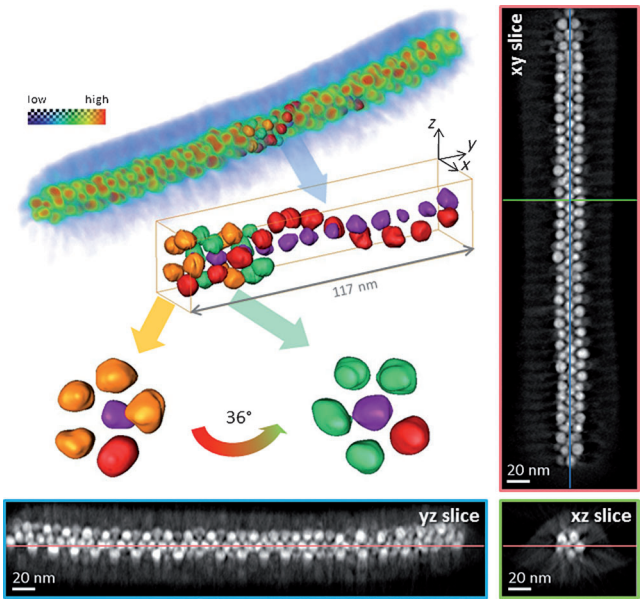

Figure 4. 3D reconstruction obtained by the tomography of AgNP packing inside the NF formed by the PS-b-P4VP block copolymer (BCP). The 3D volume rendering shows the entire structure, in which the reconstructed density is color coded according to the colorbar, that is, the AgNPs appear red (high density) and the BCP appears blue (low density). From the tomogram some of the AgNPs are segmented to visualize their spiral arrangement. The slices show sections through the center of the 3D volume in the three directions in space. The apparent shading in the slices is an artefact of the tomographic reconstruction from an incomplete tilt range, because the experimental setup allowed only a tilt range of 144° instead of 180°.

aggregates within the polymer matrix. Hence, smaller nanoparticles tend to distribute homogenously within the BCP host domain or localize at the domain interphase, whereas the larger nanoparticles segregate towards center of the domain to reduce the entropic penalty associated with chain stretching to get around the solid NPs. Balazs and co-workers[3] theoretically predicted that the nanoparticle segregation may also result in the formation of another level of superstructures formed by the nanoparticles themselves within the self-assembled BCP domains. However, such superstructures have not been found experimentally in the NP/BCP composite systems studied to date. This is not surprising since according to Balazs and co-workers,[3] these superstructures tend to exist in an extremely narrow range of diblock composition. Moreover, it was also postulated that these superstructures may be in a metastable or even unstable state and, hence, might be difficult to observe experimentally unless these metastable phases are long-lived. In the present system, the AgNPs self-assemble into an ordered superstructure and, more significantly, the packing results in a helical morphology. The formation of NP superstructures in the present system is a result of the interplay of several parameters which drive the nanoparticles to form helical packing. First of all, the volume fraction of cylinder-forming PS minority block (ca. 0.3) lies in the region in which the self-assembled helical structures of nanoparticles were predicted to exist.[3] Second, the ratio of the nanoparticle diameter (ca. 9 nm, Ag core + PS shell) with respect to the diameter of the PS cylindrical domain (ca. 40 nm) was more than 0.2 which satisfies the theoretically predicted limit for the segregation of the nanoparticles at the center of the domain. Our preliminary experiments reveal no helix formation for smaller NPs. The same arrangement occurs if the domain size of host PS cylinders is reduced, leading to the formation of irregular NP aggregates rather then ordered superstructures (see the Supporting Information for more details). Another set of parameters concerns characteristics of the AgNP-stabilizing shell. The presence of the dense PS shell is required to shield the bare AgNP surface and the P4VP chains from possible interactions, and move the nanoparticles towards the center of the PS microdomains.[7] Hence, one can expect that a decrease in PS grafting density, the nanoparticles will be driven to the PS/P4VP interphase and further to the P4VP phase. Moreover, reduced PS grafting density may lead to NP aggregation already in solution, which in turn will perturb the BCP morphology in the vicinity of large aggregates and hinder the formation of well-ordered helical assemblies. The molecular weight of the grafted polymer would also influence the helix formation. For example, in NP/homopolymer mixtures the uniform dispersion is best obtained for nanoparticles with long grafted chains, that is, "wet brush" regime, whereas in NP/BCP composites short grafted chains are preferable to prevent nanoparticles aggregation.[8] Finally, the effect of casting conditions on the formation of NP superstructures cannot be neglected.

In the past, the formation of helical structures was observed in pure ABC triblock copolymers and cylindrically confined diblock copolymers.[9] However, the helical packing of the NPs in the present case could be, more appropriately, compared to the theoretically predicted helical packing of spheres confined in a cylindrical domain. Theoretically, Pickett et al.[10] and more recently, Mughal and Chan[11] have demonstrated that the filling of uniform spherical particles into hollow cylinders may lead to remarkable sequential structures of densely packed spheres when the ratio of the cylinder diameter to that of the spheres is varied. These structures include simple chainlike and zigzag particle arrangements and also a wide spectrum of chiral and achiral particle assemblies. Experimental evidence for such packing of spheres has been found with colloids in microchannels and fullerenes in nanotubes.[12–15] However, the helical packing of NPs found in our work is the first experimental observation of the chiral packing of NPs confined in block copolymer microdomains. Even though theoretical predictions are available for this packing symmetry and our experimental results are well reproducible for this particular NP/BCP system, the exact influence of multiple parameters, both thermodynamic and kinetic, which lead to the helix formation in the present case, are not completely clear to us; further studies required to better understand plausible mechanisms are currently in progress. We suggest that with a judicious variation of parameters specific to the nanoparticle and/or block copolymer, also other superstructures of NPs resembling those predicted for the case of hard spheres packed in a cylindrical confinement, may be discovered.

In conclusion, we report the first experimental observation of a helical superstructure of closely packed AgNPs inside the cylindrical domains of a self-assembled block copolymer matrix. The present work opens up possibilities for the discovery of novel hierarchical structures in NP/BCP composite systems and also provides new opportunities for the application of such materials in nanotechnology.

Experimental Section

PS-b-P4VP BCP (M_n(PS) = 18500 g mol^{-1} and M_n(P4VP) = 40500 g mol^{-1}, PDI = 1.10) was procured from Polymer Source, Canada. The calculated volume fractions of the PS and P4VP blocks were 0.3 and 0.7, respectively. PS-stabilized silver nanoparticles were synthesized using known procedures[16] (for details on AgNP synthesis and characterization see the Supporting Information). The AgNP/PS-b-P4VP bulk composites were prepared by mixing the components in chloroform and allowing the solvent to evaporate slowly. For isolation of the AgNP-loaded individual nanofibers with PS core and P4VP shell, the bulk sample was dispersed in methanol, a selective solvent for P4VP block.[5] After ultrasonication for 15 min the NF dispersion in methanol was spin-coated/drop-cast on a silicon substrate or copper grid for further analysis.

Small-angle X-ray scattering (SAXS) measurements were performed using a Bruker Nanostar SAXS instrument. The X-ray source, a 1.5 kW X-ray generator (Kristalloflex 760) equipped with a Cu tube, was operated at 35 mA and 40 kV. The scattering intensities and patterns were detected by a two-dimensional position-sensitive detector (Bruker AXS) with 512 × 512 channels. The scattering intensities were corrected by the empty beam scattering and the sensitivity of each pixel of the 2D detector. Transmission electron microscopy (TEM) and energy-filtered TEM (EFTEM) analyses were performed on Zeiss Libra200 TEM equipped with Omega-type energy filter at 200 kV acceleration voltage. TEM imaging was done without any staining of the samples. EFTEM tomography was carried out on a Philips microscope CM200 FEG operated at 200 kV acceleration voltage with a Gatan Imaging Filter 678 (see the Supporting Information).

Received: March 24, 2014
Published online: July 2, 2014

Keywords: block copolymers · helical packing · nanoobjects · nanoparticles · self-assembly

[1] a) I. Hamley, *The Physics of Block Copolymers*, Oxford University Press, Oxford, **1998**; b) L. Leibler, *Macromolecules* **1980**, *13*, 1602 – 1617; c) F. S. Bates, G. H. Fredrickson, *Phys. Today* **1999**, *52*, 32 – 38.

[2] a) M. R. Bockstaller, R. A. Mickiewicz, E. L. Thomas, *Adv. Mater.* **2005**, *17*, 1331 – 1349; b) A. Haryono, W. H. Binder, *Small* **2006**, *2*, 600 – 611; c) M. Grzelczak, J. Vermant, E. M. Furst, L. M. Liz-Marzan, *ACS Nano* **2010**, *4*, 3591 – 3605; d) J. Kao, K. Thorkelsson, P. Bai, B. J. Rancatore, T. Xu, *Chem. Soc. Rev.* **2013**, *42*, 2654 – 2678; e) Y. Lin, A. Boker, J. B. He, K. Sill, H. Q. Xiang, C. Abetz, X. F. Li, J. Wang, T. Emrick, S. Long, Q. Wang, A. Balazs, T. P. Russell, *Nature* **2005**, *434*, 55 – 59; f) A. C. Balazs, T. Emrick, T. P. Russell, *Science* **2006**, *314*, 1107 – 1110; g) J. J. Chiu, B. J. Kim, E. J. Kramer, D. J. Pine, *J. Am. Chem. Soc.* **2005**, *127*, 5036 – 5037; h) J. Kao, P. Bai, J. M. Lucas, A. P. Alivisatos, T. Xu, *J. Am. Chem. Soc.* **2013**, *135*, 1680 – 1683; i) A. Horechyy, B. Nandan, N. E. Zafeiropoulos, P. Formanek, U. Oertel, N. C. Bigall, A. Eychmüller, M. Stamm, *Adv. Funct. Mater.* **2013**, *23*, 483 – 490.

[3] a) J. Huh, V. V. Ginzburg, A. C. Balazs, *Macromolecules* **2000**, *33*, 8085 – 8096; b) R. B. Thompson, V. V. Ginzburg, M. W. Matsen, A. C. Balazs, *Macromolecules* **2002**, *35*, 1060 – 1071; c) R. B. Thompson, V. V. Ginzburg, M. W. Matsen, A. C. Balazs, *Science* **2001**, *292*, 2469 – 2472.

[4] a) Z. Y. Fan, A. O. Govorov, *Nano Lett.* **2010**, *10*, 2580 – 2587; b) A. Guerrero-Martínez, B. Auguié, J. L. Alonso-Gomez, Z. Dzolic, S. Gómez-Grana, M. Zinic, M. M. Cid, L. M. Liz-Marzán, *Angew. Chem.* **2011**, *123*, 5613 – 5617; *Angew. Chem. Int. Ed.* **2011**, *50*, 5499 – 5503; c) A. Kuzyk, R. Schreiber, Z. Y. Fan, G. Pardatscher, E. M. Roller, A. Hogele, F. C. Simmel, A. O. Govorov, T. Liedl, *Nature* **2012**, *483*, 311 – 314; d) S. Droulias, V. Yannopapas, *J. Phys. Chem. C* **2013**, *117*, 1130 – 1135.

[5] J. Pal, S. Sanwaria, R. Srivastava, B. Nandan, A. Horechyy, M. Stamm, H. L. Chen, *J. Mater. Chem.* **2012**, *22*, 25102 – 25107.

[6] P. A. Midgley, R. E. Dunin-Borkowski, *Nat. Mater.* **2009**, *8*, 271 – 280.

[7] B. J. Kim, J. Bang, C. J. Hawker, E. J. Kramer, *Macromolecules* **2006**, *39*, 4108 – 4114.

[8] a) C. Xu, K. Ohno, V. Ladmiral, D. E. Millkie, J. M. Kikkawa, R. J. Composto, *Macromolecules* **2009**, *42*, 1219 – 1228; b) C. Xu, K. Ohno, V. Ladmiral, R. J. Composto, *Polymer* **2008**, *49*, 3568 – 3577.

[9] U. Krappe, R. Stadler, I. Voiget-Martin, *Macromolecules* **1995**, *28*, 4558 – 4561; b) P. Dobriyal, H. Xiang, M. Kazuyuki, J.-T. Chen, H. Jinnai, T. P. Russell, *Macromolecules* **2008**, *42*, 9082 – 9088.

[10] G. T. Pickett, M. Gross, H. Okuyama, *Phys. Rev. Lett.* **2000**, *85*, 3652 – 3655.

[11] a) A. Mughal, H. K. Chan, D. Weaire, *Phys. Rev. Lett.* **2011**, *106*, 115704; b) H. K. Chan, *Phys. Rev. E* **2011**, *84*, 050302; c) H. K. Chan, D. Weaire, S. Hutzler, A. Mughal, *Phys. Rev. E* **2012**, *85*, 051305.

[12] Y. D. Yin, Y. N. Xia, *J. Am. Chem. Soc.* **2003**, *125*, 2048 – 2049.

[13] M. Tymczenko, L. F. Marsal, T. Trifonov, I. Rodriguez, F. Ramiro-Manzano, J. Pallares, A. Rodriguez, R. Alcubilla, F. Meseguer, *Adv. Mater.* **2008**, *20*, 2315 – 2318.

[14] A. N. Khlobystov, D. A. Britz, A. Ardavan, G. A. D. Briggs, *Phys. Rev. Lett.* **2004**, *92*, 245507.

[15] L. X. Jiang, J. W. J. de Folter, J. B. Huang, A. P. Philipse, W. K. Kegel, A. V. Petukhov, *Angew. Chem.* **2013**, *125*, 3448 – 3452; *Angew. Chem. Int. Ed.* **2013**, *52*, 3364 – 3368.

[16] H. Hiramatsu, F. E. Osterloh, *Chem. Mater.* **2004**, *16*, 2509 – 2511.

